Universal short-time dynamics in the Kosterlitz-Thouless phase

P. Czerner and U. Ritschel
Fachbereich Physik, Universität GH Essen, 45117 Essen, Federal Republic of Germany
(Received 12 October 1995)

We study the short-time dynamics of systems that develop quasi-long-range order after a quench to the Kosterlitz-Thouless phase. With the working hypothesis that the universal short-time behavior, previously found in Ising-like systems, also occurs in the Kosterlitz-Thouless phase, we explore the scaling behavior of thermodynamic variables during the relaxational process following the quench. As a concrete example, we investigate the two-dimensional six-state clock model by Monte Carlo simulation. The exponents governing the magnetization, the second moment, and the autocorrelation function are calculated. From them, by means of scaling relations, estimates for the equilibrium exponents z and η are derived. In particular, our estimates for the temperature-dependent anomalous dimension η that governs the static correlation function are consistent with existing analytical and numerical results, and, thus, confirm our working hypothesis.

PACS number(s): 64.60.Ht, 75.40.Gb, 67.40.Fd, 02.70.Lq

I. INTRODUCTION

As discovered by Janssen *et al.* [1], universal short-time behavior (USTB) in critical dynamics occurs after quenching a spin system with nonconserved order parameter (model A [2]) from a high-temperature initial state to its critical point. In its most pronounced form the USTB manifests itself in the time dependence of the order parameter. Starting from a small average initial magnetization m_0, the order starts to grow during a nonequilibrium (though universal) stage shortly after the quench, before the decay to the equilibrium value zero sets in. The initial increase is governed by a power law

$$m \sim m_0 t^{\theta} \tag{1.1a}$$

and the short-time exponent θ is given by [3,4]

$$\theta = \frac{\eta_0 - \eta}{2z}, \tag{1.1b}$$

i.e., it is determined by the difference between the anomalous dimensions η_0 and η of the *initial* order-parameter field and the equilibrium magnetization, respectively. (z denotes the dynamic equilibrium exponent.) θ (or, equivalently η_0) is a new exponent, not expressible in terms of known static and/or dynamic exponents [1]. Thus the initial increase will only occur under the condition that $\eta_0 > \eta$, which, for instance, is fulfilled in the case of the Ising model for spatial dimensions $1 < d < 4$.

Recently significant progress has been made in quantitative studies of the USTB by means of Monte Carlo (MC) simulations. It turned out to be possible to observe the short-time power law (1.1a) in surprisingly small systems and after relatively short simulation times [5,6]. As the exponents governing the short-time behavior of thermal averages can be expressed in terms of scaling relations among short-time and equilibrium exponents, it is possible to extract even static exponents from a relatively early stage of the dynamics, whereby the problem of critical slowing down is circumvented to some extent [7,8].

As pointed out by Janssen [9], the qualitative mechanism underlying the USTB is the following. After the quench the initially small correlation length starts to grow towards its equilibrium value. During the early stages, when fluctuations are still short ranged, a mean-field description of the process should hold. Since in Ising-like systems T_c^{MF} is always larger than the real T_c, it is plausible that shortly after the quench a spontaneous magnetization will evolve, pointing in the direction of the initial magnetization m_0. At some point, when $\xi(t)$ has grown to a certain size, this increase will come to a halt, and afterwards the decay to the equilibrium value $m(t \to \infty) = 0$ will begin.

So far, in both analytical and numerical calculations the USTB has only been studied in Ising-like systems, with a conventional critical (or tricritical) point [1,3,5–11]. However, the phenomenon should not only occur at a critical point, but, more generally, in situations where scale-invariant long-ranged fluctuations evolve after a quench from a high-temperature initial state (or after any other comparable change of the state of the system). In the following this scenario is tested for a quench to the Kosterlitz-Thouless (KT) phase. In two-dimensional systems with O(2) symmetry (or variants of it) below the KT transition temperature T_{KT}, one finds a range of temperatures with a power-law decay of the static correlation function [12,13]. Examples are the XY model and the p-state clock model for $p \geq 5$. Additionally, mean-field theory predicts for these systems (erroneously) a conventional critical point, and one finds generally $T_c^{\mathrm{MF}} > T_{\mathrm{KT}}$. Thus, taking into account the foregoing discussion, the USTB should also be observable after a quench to the KT phase, and it is interesting to see whether the methods described in Refs. [5–8] can be applied, i.e., whether, for instance, the equilibrium exponent η can be extracted from the short-time relaxational behavior.

The rest of this paper is organized as follows. In the next section we recall analytical and numerical results for the clock model. In Sec. III we derive the scaling behavior of the relevant thermodynamic quantities, taking into account the anomalous scaling of the initial magnetization. Our own simulations have been carried out for the $p = 6$ clock model. The numerical results are presented in Sec. IV.

II. THE CLOCK MODEL

According to the Mermin-Wagner theorem [14], the two-dimensional XY model cannot undergo a conventional para- to ferromagnetic phase transition. However, as shown by Kosterlitz and Thouless [12], there exists a transition between a state with unbounded and bounded vortices at $T = T_{\mathrm{KT}}$.

A model that in many respects interpolates between the Ising model and the XY model is the p-state clock model, defined by the Hamiltonian

$$H = -J \sum_{\langle ij \rangle} \vec{s}_i \cdot \vec{s}_j = -J \sum_{\langle ij \rangle} \cos(\vartheta_i - \vartheta_j) ,$$

$$\vartheta_i = \frac{2\pi}{p} n_i , \tag{2.1}$$

where $n_i \in \{0, 1, \ldots, p-1\}$ and $\langle\,\rangle$ denotes the sum over nearest neighbors. This spin system is equivalent to the XY model for $p \to \infty$ and to the Ising model for $p = 2$. It was first shown by Jose *et al.* [13] and later on verified by numerous MC studies [15–20] that the p-state clock model has a single Ising-like critical point for $p \leq 4$. For $p \geq 5$, on the other hand, there exist two transition points, with temperatures T_1 and T_2 ($> T_1$), respectively. For $T > T_2$ a paramagnetic high-temperature phase exists and for $T < T_1$ the system becomes ferromagnetic. For $T_1 < T < T_2$, however, a KT phase with "quasi-long-range order" emerges, where the static spin-spin correlation function behaves as $C(\mathbf{r}) \sim |\mathbf{r}|^{-\eta}$, with the anomalous dimension $\eta = \eta(T)$ continuously depending on the temperature [13]. Both transitions are of KT type, i.e., the correlation length diverges exponentially as T_1 (T_2) is approached from below (above) [13].

Our MC simulations—the results are presented in Sec. IV—were done for the ($p = 6$)-state clock model. The case $p = 6$ was studied in great detail in the literature, partly motivated by the fact that in real two-dimensional systems one expects anisotropies with sixfold symmetry due to the lattice structure [13]. Approximate analytic results for the transition temperatures and the exponent $\eta(T)$ have been obtained by Jose *et al.* [13]. While T_2 was found to be identical to the KT transition temperature of the XY model, $T/J = 0.95$, T_1 was predicted to vary as $T_1/J = 4\pi^2/1.7p^2$ [which means $T_1/J = 0.645$ for $p = 6$]. (Here and in the following we set the Boltzmann constant $k_B = 1$.) The exponent η was found to vary between $\eta(T_2) = 1/4$ and $\eta(T_1) = 4/p^2$ [which means $\eta(T_1) = 0.111$ for $p = 6$].

Among the MC analyses mentioned above, we used the results of Challa and Landau [18] for comparison with our own data. They found for the transition temperatures $T_2/J = 0.92(1)$ and $T_1/J = 0.68(2)$ and for the corresponding exponents $\eta(T_2) = 0.275$ and $\eta(T_1) = 0.100$. [No error bars for $\eta(T)$ are given in Ref. [18].] The results for both the transition temperatures and the exponents are consistent with the analytic results of Ref. [13].

Dynamic MC simulations for the six-state clock model were performed by Kaski *et al.* [17], but in this work the relaxational behavior in the ferromagnetic phase was studied, with emphasis on the growth of the domain size after a quench. Thus, concerning the temperature ranges, this work is complementary to ours.

In order to comply with the requirements for the occurrence of the USTB discussed in the Introduction, the system has to have a mean field T_c^{MF} above the temperature to which the quench is carried out. In the case of the clock model it is straightforward to show that there exists a T_c^{MF} for all $p \geq 2$ and that $T_c^{\mathrm{MF}}/J = 2d$ for $p = 2$ (Ising case) and $T_c^{\mathrm{MF}}/J = d$ for $p > 2$, where d denotes the spatial dimension. A comparison with exact or numerical results for the clock models shows that the upper transition temperature (which is a critical point for $p = 2, 3, 4$) is below T_c^{MF} for all $p \geq 2$. For example, for $p = 6$, the upper transition temperature $T_2/J \simeq 0.92$ is well below $T_c^{\mathrm{MF}}/J = 2$.

III. SCALING ANALYSIS

In the KT phase, i.e., for all temperatures below T_{KT}, the bulk *equilibrium* correlation length is infinite. After a sudden quench from a high-temperature initial state to the KT phase, the initially small correlation length $\xi(t)$ starts to grow and the large-scale fluctuations gradually develop. Let us first discuss relaxational processes in Ising-like systems. In this case, after a short period of nonuniversal behavior following the quench, the growth of the correlation length is described by the universal power law

$$\xi(t) \sim t^{1/z} , \tag{3.1}$$

and in the bulk system $\xi(t)$ becomes "macroscopic" for large times. Moreover, in the regime of universal behavior $\xi(t)$ is the *only* macroscopic time scale and allows us to characterize the time dependence of correlation functions completely. In the finite systems, (3.1) holds as long as $\xi(t) < L$ (where L is the linear system dimension). In the following this scenario will be called simple (dynamic) scaling.

In the KT phase vortices are generated in the course of the quench and potentially disturb the simple scaling picture [21–23]. Deviations from the simple scaling picture are expected mainly for intermediate times. As we shall see from the evaluation of the MC data, modifications compared to the Ising dynamics really occur in certain quantities in form of a relatively slow approach to the power-law form. Below we review the simple scaling scenario concerning the quantities studied in our MC simu-

lation, with emphasis on the (expected) consequences of the USTB. Modifications due to vortices are discussed in some more detail in the context of the MC simulation in Sec. IV.

A. Bulk behavior

Consider first the expectation value of the magnetization density [24]. Suppose in the high-temperature initial state an external magnetic field has generated a small (initial) magnetization m_0, pointing in the $\vartheta = 0$ direction of the xy plane. Then, after the quench, the expectation value of the order parameter, defined by

$$m(t) := L^{-2} \left\langle \sum_i \cos \vartheta_i \right\rangle , \tag{3.2}$$

should remain in the direction of the initial magnetization. In the scaling regime it should further satisfy the homogenity property [25]

$$m(t, m_0) \approx l^{\eta/2}\, m(l^z t,\, l^{-\eta_0/2} m_0) , \tag{3.3}$$

where l is a rescaling parameter and the exponents η, η_0 were introduced in Eq. (1.1).

From Eq. (3.3) it follows that, asymptotically, the magnetization behaves as

$$m(t, m_0) \sim t^{-\eta/2z}\, \mathcal{F}(m_0\, t^{\eta_0/2z}) , \tag{3.4}$$

where $\mathcal{F}(x)$ is a universal scaling function. As an immediate consequence of $\eta_0 \neq \eta$ in Eq. (3.3), the rescaled (or renormalized) m_0 is no longer the initial value of $m(t)$. However, one still has asymptotically $m \propto m_0$ for $t \to 0$ [1,9]. Thus the scaling function $\mathcal{F}(x)$ in (3.4) is proportional to x for $x \to 0$ and, as a result, the short-time behavior is described by (1.1).

Further, from the combination in the argument of $\mathcal{F}$ in (3.4) one realizes that m_0 also gives rise to a time scale $t_0 \sim m_0^{-2z/\eta_0}$. While for $t \lesssim t_0$ the USTB (1.1a) is observed, the system crosses over to the nonlinear decay $m \sim t^{-\eta/2z}$ for $t \gtrsim t_0$, which implies that $\mathcal{F}(x) \to$ const for $x \to \infty$ and that memory of the initial value m_0 is lost for $t \gg t_0$.

Can we expect to observe the USTB even for $m_0 = 0$? Obviously, in this case the magnetization vanishes identically for $t > 0$. However, as demonstrated in Ref. [9], the USTB leaves its mark on the relaxational behavior of the autocorrelation function

$$A(t) = \langle \vec{s}_i(t) \cdot \vec{s}_i(0) \rangle , \tag{3.5}$$

which measures the change the system has undergone during the time t after the quench. Without going into the technical details, here we present just Janssen's result [9]

$$A(t) \sim t^{-\lambda/z} \qquad \text{with} \quad \lambda = 2 - z\theta , \tag{3.6}$$

i.e., the short-time exponent θ also appears in $A(t)$ and leads to a deviation from the naive expectation $\lambda = 2$, surprisingly for all $t > 0$. It was this quantity where the USTB actually was first observed in a MC simulation [26].

The third quantity that will play a role in the following is the second moment (or variance) of the magnetization. It is defined by

$$m^{(2)}(t) = L^{-2} \left\langle \sum_{i,j} \vec{s}_i(t) \cdot \vec{s}_j(t) \right\rangle . \tag{3.7}$$

A straightforward analysis reveals that $m^{(2)}(t)$, again for vanishing initial magnetization, takes the scaling form

$$m^{(2)}(t) \sim t^b \qquad \text{with} \quad b = \frac{2-\eta}{z} , \tag{3.8}$$

i.e., the USTB does not influence this quantity [27].

As suggested by Schülke and Zheng [8], the three exponents θ, λ, and b, governing the bulk behavior of m, A, and $m^{(2)}$, respectively, suffice to determine the *equilibrium* quantities η and z from the USTB. The starting point is the short-time exponent itself, which can be obtained from simulations with small, nonvanishing m_0. Then, from simulations with $m_0 = 0$, the exponents λ and b can be estimated simultaneously. Utilizing the scaling relation (3.6), z can be determined and, in turn, with relation (3.8) eventually the scaling dimension η.

Our main hypothesis for the present work is that also in the KT phase, by analogy with the situation in the critical Ising model, the operator dimension of the initial field η_0 is different from η and that, as a consequence, the scaling picture developed above also describes the short-time dynamics in the KT phase. This is neither obvious nor by any means rigorously proved. At the present stage it is merely a working hypothesis, which below will be tested by means of MC simulations. Especially for quenches to the KT phase, we expect all exponents to depend on the respective final temperature to which the quench is carried out.

B. Finite-size scaling

Starting from Eq. (3.3), all the results about the scaling behavior of the thermodynamic quantities described so far hold in the bulk system. If we are dealing with a system of finite size—and certainly this is the case in the MC simulation—the power laws (1.1a), (3.6), and (3.8) hold as long as the time-dependent correlation length $\xi(t) \sim t^{1/z}$ is smaller than the system size L. A finite-size scaling analysis reveals how the thermodynamic quantities behave during the later stages of the relaxational process [3,28].

Taking into account the finite system size, the analog to (3.3) reads

$$m(t, m_0, L) \approx l^{\eta/2} m(l^z t, l^{-\eta_0/2} m_0, lL) . \tag{3.9}$$

Removing the rescaling parameter l by setting $l \sim L$, one obtains

$$m(t, m_0, L) \sim L^{-\eta/2}\, \mathcal{G}(t/L^z, m_0 L^{\eta_0/2})\,, \qquad (3.10)$$

where $\mathcal{G}(x,y)$ is a universal scaling function. As seen from (3.10), the size L of the system gives rise to another characteristic time scale $t_L \sim L^z$ (besides the initial time scale t_0), the well-known finite-size scale [29]. In the KT phase it turns out to be temperature dependent. Further, it was shown in Ref. [3] that $\mathcal{G}(x,y) \sim \mathcal{A}(y)e^{-x}$ for $x \to \infty$, i.e., the magnetization decays exponentially when $t \gg L^z$. The scaling function $\mathcal{A}(y)$ in (3.10) describes the universal dependence during the late stages of the relaxational process on the initial magnetization m_0. This dependence is special to the finite-size system [28]. In the bulk memory of the initial condition is lost for $t \to \infty$.

For arbitrary x and $y \to 0$, the function $\mathcal{G}(x,y)$ behaves as $\mathcal{G} \sim y\,\mathcal{B}(x)$, with a scaling function $\mathcal{B}$. In this limit the maximum of the magnetization profile has the scaling form

$$m_{\max} \sim L^{(\eta_0-\eta)/2}\, m_0\, \mathcal{B}(t_{\max}/L^z)\,. \qquad (3.11)$$

Thus the finite-size scaling behavior of $m_{\max}$ allows us in principle to determine *directly* the difference $\eta_0 - \eta$.

Also for the other quantities discussed in Sec. III A the asymptotic behavior is modified when $\xi(t) \gtrsim L$. First, the autocorrelation function (3.5) also decays exponentially for $t \gtrsim t_L$. Second, the second moment takes the scaling form

$$m^{(2)}(t, L) \sim t^b\, \mathcal{J}(t/t_L). \qquad (3.12)$$

In order to reproduce (3.8), the scaling function $\mathcal{J}(x)$ has to approach a constant for $x \to 0$. For $x \to \infty$, $\mathcal{J}(x) \sim x^{-b}$, such that in the long-time limit the equilibrium result $m^{(2)} \sim L^{2-\eta}$ is obtained. Again, in the KT phase we expect to observe the finite-size scaling scenario presented above, with the characteristic scale t_L depending on the temperature.

IV. MONTE CARLO ANALYSES

A. Method

We used the usual time-dependent interpretation of the sampling algorithm [30], with sequential updating and nonconserved total spin. We employed the heat-bath algorithm, as described in detail for the clock model in Ref. [20]. It is equivalent to Glauber dynamics [30]. All simulations were carried out on square lattices with varying linear dimension L with periodic boundary conditions.

As the initial configurations we used equilibrium states for uncoupled spins in an external magnetic field $h = 2m_0$ (with $m_0 = 0$ for the autocorrelation function and the second moment). Time-dependent thermal averages were approximated by summing over a number of N histories, N varying between 1000 and 10 000 depending on the size L. In order to obtain a measure for the error, the N histories were divided in 10–20 runs, from which statistically independent exponent "measurements," their mean value, and the statistical error of the mean value were obtained.

As mentioned in the Introduction, an attractive feature of the USTB in Ising-like systems is that relatively small lattices and short simulation times turned out to be sufficient to extract reliable results for exponents [5,7,8]. However, the estimates obtained will in general to some extent depend upon the lattice size L and, in the case of θ, upon the initial magnetization m_0. In the case of the clock model, it turned out that one has to go to somewhat larger lattices and, especially in the case of the autocorrelation function, the time until the power-law behavior is assumed is increased compared to the Ising or Potts model.

B. The short-time exponent θ and the linear relaxation time

First we discuss our data for the magnetization and the determination of the short-time exponent θ from them. In order to get an impression of the time dependence of the order parameter, we have calculated relaxation profiles of the six-state clock model for $L = 30$ and $m_0 = 0.05$ in the temperature range $0.5 \le T/J \le 1.1$, i.e., the lower limit lies well below T_1 in the ferromagnetic phase and the upper limit above T_2 in the paramagnetic phase.

The results are displayed in semilogarithmic form in Fig. 1 and in double-logarithmic form in Fig. 2. For temperatures $T/J \lesssim 1.1$ the magnetization has the tendency to increase initially. For the highest temperature represented in the figure, this increase lasts only for about 10–20 updates of the lattice, but it becomes more and more pronounced at lower temperatures. As one can see from Fig. 2, a clearly identifiable initial power-law regime at about $10 \lesssim t \lesssim 100$ can be observed for $T/J \lesssim 0.95$. (The time is always given in Monte Carlo steps per spin.)

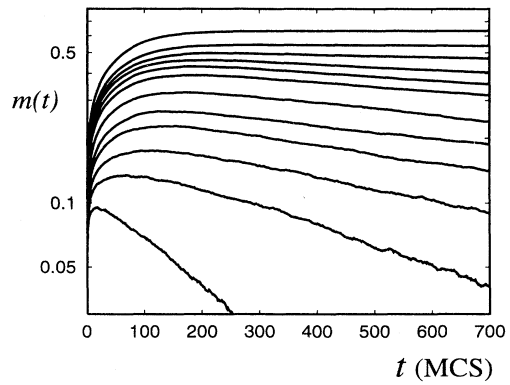

FIG. 1. Magnetization of the six-state clock model as a function of time [in units of Monte Carlo steps (MCS) per spin] in a semilogarithmic representation for $L = 30$ and $m_0 = 0.05$ for various temperatures in, below, and above the KT phase. From bottom to top the corresponding temperatures are $T/J = 1.1, 1.04, 1.0, 0.95, 0.92, 0.84, 0.76, 0.72, 0.68, 0.64, 0.6$, and 0.5.

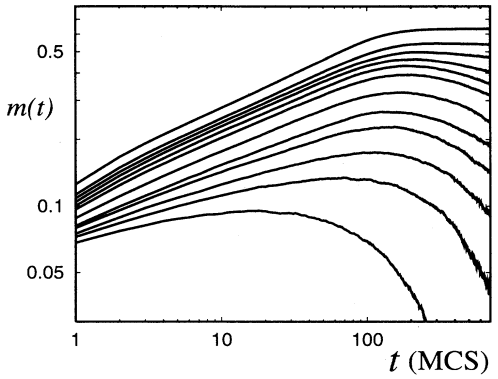

FIG. 2. Same profiles as in Fig. 1 in a double-logarithmic representation, emphasizing the initial power-law growth of the magnetization.

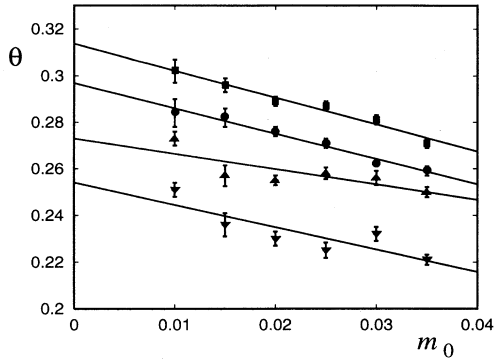

FIG. 4. Results for the short-time exponent θ as a function of m_0 for four temperatures $T/J = 0.68$ (squares), 0.76 (full circles), 0.84 (triangles), and 0.92 (inverted triangles). The respective linear fits, from which the extrapolations to $m_0 = 0$ were obtained, are also displayed.

All curves in the temperature range $0.64 \lesssim T/J \lesssim 1.1$ have a maximum and thereafter decay exponentially or "linearly" $\sim e^{-t/t_L}$.

It is instructive to extract the linear relaxation time t_L from the data in Fig. 1. It depends on both the system size and the temperature; results for $t_L(T)$ for $L = 30$ are displayed in Fig. 3 (squares for $p = 6$). The temperature range of the KT phase as obtained by Challa and Landau [18] is indicated in the figure. Obviously, the KT phase manifests itself as a plateaulike structure in this quantity, roughly located between T_1 and T_2 of Ref. [18]. Coming from the high-temperature side, t_L increases up to about $T/J = 0.95$. Then t_L remains almost unchanged down to $T/J = 0.75$ and starts to grow rapidly when going to lower temperatures. For $T/J \lesssim 0.6$ the magnetization approaches more or less a constant within the observation time $t < 1200$, which means that t_L becomes effectively infinite. The latter is due to an exponentially growing tunneling time in the ferromagnetic phase [30].

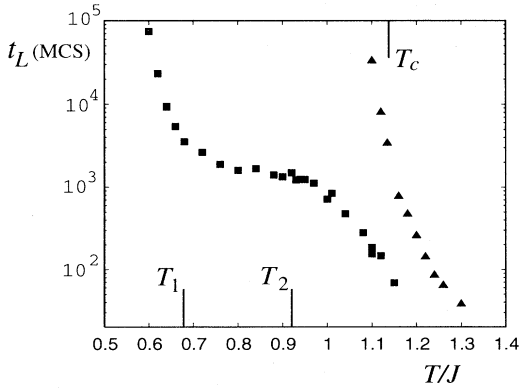

FIG. 3. Linear relaxation times t_L for $p = 6$ (squares) and $p = 4$ (triangles) as a function of temperature for $L = 30$ and $m_0 = 0.05$. Both the (exact) critical temperature of the four-state clock model, $T_c/J = 1.13\ldots$, and the upper and lower transition temperatures $T_1/J = 0.68$ and $T_2/J = 0.92$ determined Challa and Landau [18] are indicated in the figure. The error bars are approximately of the same size as the symbols.

For comparison we calculated a number of curves for the four-state clock model in the vicinity of its (exact) critical temperature $T_c/J = 1.1345\ldots$. The corresponding linear relaxation time is also shown in Fig. 3 (circles). It is steadily increasing for decreasing temperature, as one would have expected in the vicinity of a critical point, and no plateau is seen.

In order to determine the short-time exponent θ, we calculated magnetization profiles for the lattice size $L = 300$. As also found for other models [8], the outcome for the short-time exponent θ varies significantly with m_0. From the renormalization-group analysis it is clear [1,3] that the pure scaling form (1.1a) is assumed for $m_0 \to 0$ only. Unfortunately, it is hard to obtain reliable results for θ in this limit, as for $m_0 = 0$ the signal vanishes completely, and for decreasing m_0 it becomes more and more blotted out by the noise. Hence, as in Ref. [8], we calculated profiles for a number of initial values m_0 and then determined θ by fitting a power law to the short-time regime. As the fit interval we chose [10, 300]. The results for θ as a function of m_0 for the temperatures $T/J = 0.6$, 0.68, 0.76, 0.84, and 0.92 are shown in Fig. 4. The values of the short-time exponent obtained by extrapolating linear fits to $m_0 = 0$ are listed in Table I.

Some representative profiles for $L = 300$ and $m_0 = 0.01$ are presented in Fig. 5 (solid lines). They show that in the given temperature range the initial increase is consistent with a power law. As seen from the other curves displayed in Fig. 5, this is drastically different at low temperatures. For example, for $T/J = 0.2$ (upper dashed curve), deep in the ferromagnetic regime, the time dependence of the magnetization is more complicated and only for $t \gtrsim 200$ power-law behavior is assumed. This is weakly indicated already at $T/J = 0.6$ (lower dashed line).

C. The autocorrelation function and the exponent λ

The autocorrelation function $A(t)$ as defined in Eq. (3.5) is governed by the exponent λ/z. Exemplary re-

TABLE I. Monte Carlo estimates for the exponents of the two-dimensional six-state clock model for temperatures within and slightly below the KT phase. For comparison the respective exponents of the critical Ising model (at $T_c/J = 2.2691\ldots$) are also displayed. In the latter case θ and z were taken from Ref. [6], and λ/z, b, and $\eta_0 - \eta$ were obtained with the help of (3.6), (3.8), and (1.1b) using the exact $\eta = 0.25$.

T/J	θ	λ/z	b	z	η	$\eta_0 - \eta$
0.92	0.254(5)	0.670(10)	0.816(12)	2.16(4)	0.23(6)	1.10(3)
0.84	0.273(6)	0.644(19)	0.832(10)	2.18(6)	0.19(7)	1.19(4)
0.76	0.297(2)	0.622(11)	0.842(12)	2.18(3)	0.17(5)	1.29(2)
0.68	0.314(2)	0.577(6)	0.856(11)	2.24(2)	0.08(4)	1.41(2)
0.60	0.355(5)	0.517(6)	0.838(11)	2.29(3)	0.08(5)	1.63(3)
Ising	0.191(2)	0.730(6)	0.806(2)	2.172(6)	0.25	0.83(1)

sults for $A(t)$ in the KT phase for $L = 300$ (and $m_0 = 0$) are displayed in Fig. 6 (solid lines). Even from this representation one can tell that the curves are slightly curved up to $t \simeq 100 - 200$ and that they approach a power law, if at all, only relatively slowly. This is the reason why the exponent λ/z in (3.6) cannot be determined on smaller lattices with, say, $L = 100$. In this case $A(t)$ crosses over to the finite-size (linear) decay before a reliable estimate for λ/z can be extracted. For comparison we have also plotted the autocorrelation function for the critical Ising model in Fig. 6 (dashed curve).

In order to overcome this obstacle, we calculated the autocorrelation function for $L = 300$ up to $t = 1000$. Then λ/z was determined by fitting the data in an interval $[t_1, t_2]$ within the power-law regime. To determine the minimal t_1 (called delay time in the following), we calculated the difference ΔA between the data and the fit for a given interval. While the upper limit $t_2 \simeq 1000$ was fixed, the lower limit t_1 was increased until (besides random fluctuations) ΔA did not show any systematic deviation from the fit within $[t_1, t_2]$.

Consider first the temperature $T/J = 0.68$. Numerical results for ΔA are shown in Fig. 7 (two upper curves). For the uppermost curve the fit interval was $[200, 1000]$. It is obvious that, besides the random short-scale fluctuations, the data systematically deviate from the fitted power law; for $200 \lesssim t \lesssim 300$ the data are below and for $400 \lesssim t \lesssim 600$ they are systematically above zero. In contrast, a fit to the interval $[500, 1000]$ (second curve from above in Fig. 7) shows no systematic deviation and thus, for this temperature, the power-law regime seems to be reached for $t \simeq 500$.

In Fig. 7 we have also plotted $\Delta A(t)$ for the critical Ising model with fit interval $[80, 1000]$. Although the delay time $t_1 \simeq 80$ is much shorter than for the clock model, it is still relatively large compared with $m(t)$ or $m^{(2)}(t)$, where one finds power-law behavior for $t \gtrsim 10$.

In Fig. 8 the difference $\Delta A(t)$ is displayed for various temperatures within and below the KT phase. The estimated delay times are 500, 400, 500, 650, 450, and 200 for $T/J = 0.2$, 0.6, 0.68, 0.76, 0.84, and 0.92, respectively. Thus t_1 is relatively short at T_2, increases when T is decreasing, and appears to become smaller again for $T \lesssim T_1$. However, presently our data are not accurate enough to allow for definite statements about the temperature dependence of t_1.

The results for λ/z are shown in Table I. The slow approach the power-law behavior of $A(t)$ is a feature not

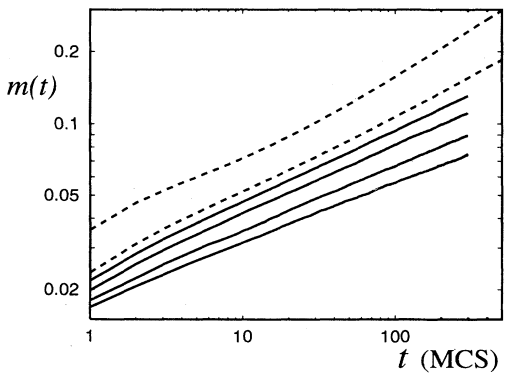

FIG. 5. Initial behavior of the order parameter for $L = 300$ and $m_0 = 0.01$ for (from bottom to top) $T/J = 0.92$, 0.84, 0.76, 0.68, 0.6, and 0.2. The solid curves represent profiles within the KT phase.

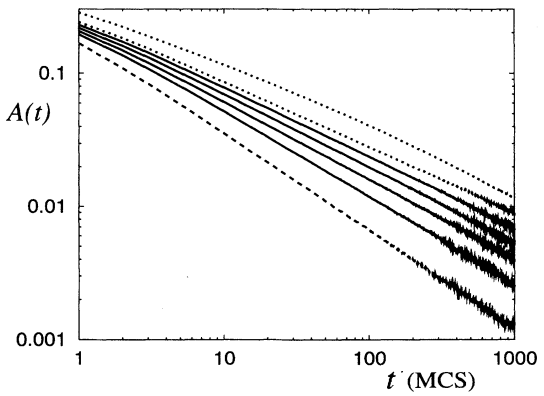

FIG. 6. Autocorrelation function defined in (3.5) for $L = 300$ and $m_0 = 0$ for $T/J = 0.92$, 0.84, 0.76, 0.68, 0.6, and 0.2 (upper six curves from bottom to top). The dashed curve represents the data for the critical Ising model.

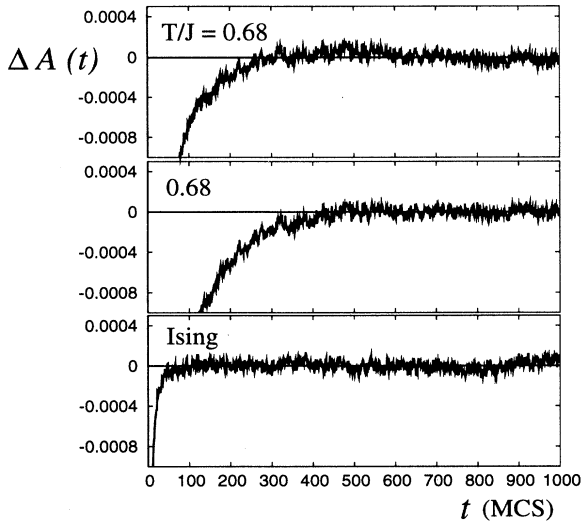

FIG. 7. Difference $\Delta A(t)$ between the data for the autocorrelation function and the power-law fit obtained for $T/J = 0.68$ and fit intervals $[200, 1000]$ (upper curve) and $[500, 1000]$ (middle curve). The bottom curve shows ΔA for the critical Ising model and fit interval [80,1000].

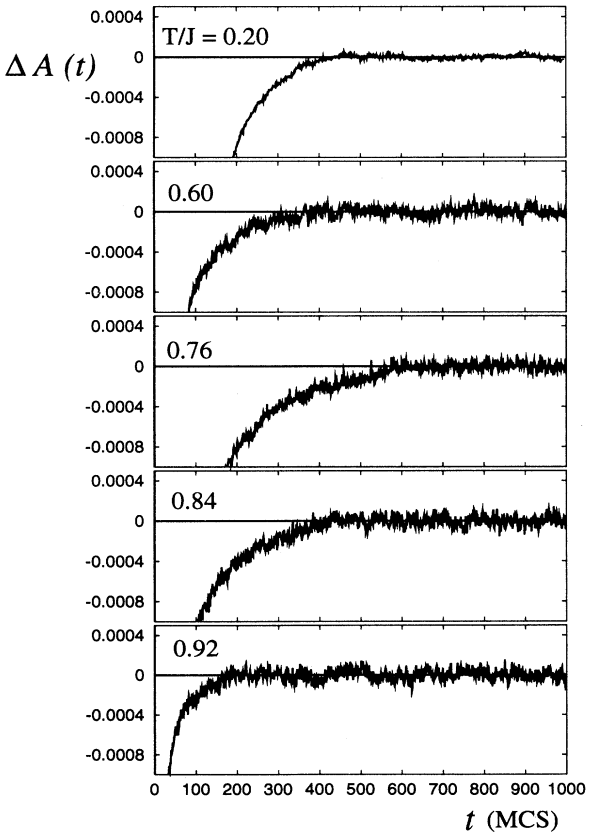

FIG. 8. $\Delta A(t)$ for $T/J = 0.92$, 0.84, 0.76, 0.6, and 0.2; the respective fit intervals are [200,1000], [450,1000], [650,1000], [400,1000], and [500,1000].

seen in the Ising model. Presumably it is due to vortices that are abundantly generated during the quench and slowly annihilate during the ensuing relaxation. The influence of vortices on the dynamics of the XY model was discussed by several authors in the literature. Vortices in general give rise to new length scales [21,23] and, as a consequence, the simple scaling picture discussed in Sec. II breaks down. It was also shown that in certain quantities a slow (logarithmic) approach to the power-law behavior occurs [21,22], especially in those that are substantially influenced by short-wavelength fluctuations of the order-parameter field. However, with the help of the existing literature it was not possible for us to get a complete understanding of the observed dynamics at intermediate time scales. Because we were mainly interested in the asymptotic power laws and the exponents governing them, we did not pursue this point any further.

D. The second moment and results for z and η

The short-time behavior of the second moment $m^{(2)}(t)$ defined in (3.7) is much less problematic than that of $A(t)$. Some representative curves are shown in Fig. 9. As before, the results for the KT phase are the solid curves. The power-law behavior is found for $t \gtrsim 20$ and the exponent b in (3.8) was determined in the interval $[20, 500]$. The results are listed in Table I.

Obviously, b and because of (3.8) the combination $(2-\eta)/z$ do not depend much on the temperature. Taking into account the error bars, the outcome is even consistent with a temperature-independent exponent, although a weak decrease for increasing temperature seems also possible.

As can be further seen from Fig. 9 also for the critical Ising model (dashed curve), this exponent is not much different. From our own data displayed in Fig. 9 we determined $b = 0.81(1)$. Taking alternatively the exact $\eta = 0.25$ and the literature value $z = 2.172(6)$ [6], one finds, with the help of (3.8), $b = 0.806(2)$. Finally, we

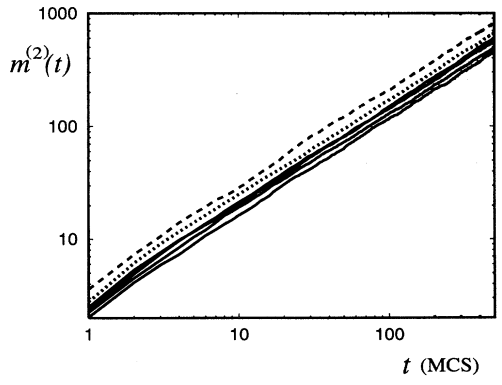

FIG. 9. Second moment defined in (3.7) for $L = 300$, $m_0 = 0$, and $T = 0.92$, 0.84, 0.76, 0.68, and 0.6 (lower five curves from bottom to top). The dashed curve shows the data for the critical Ising model.

use the scaling relation (3.6) and (3.8) to get estimates for the dynamic exponent $z(T)$, the anomalous dimension $\eta(T)$, and the difference $\eta_0 - \eta$. The results are also displayed in Table I.

V. SUMMARY AND DISCUSSION

We investigated the short-time relaxational behavior of the two-dimensional clock model after a quench from a high-temperature initial state to the KT phase. Motivated by the situation in Ising-like systems, we assumed that an independent initial exponent also exists for the clock model, that it determines the short-time behavior in the KT phase, and that the static exponent $\eta(T)$ can be determined from the initial stage of relaxation processes. Under the assumption that the dynamics is asymptotically governed by only one (macroscopic) length scale, the time-dependent correlation length $\xi(t) \sim t^{1/z}$, we explored the consequences of the anomalous short-time behavior. Numerical results for the magnetization, its second moment, and the autocorrelation function were obtained by Monte Carlo simulation.

A feature that is not found in the Ising model is a relatively slow approach to a power law of the autocorrelation function. Presumably, this is due to vortices and additional length scales associated with them. From the existing literature we were not able to get a full quantitative understanding of this phenomenon, in particular in view of the relatively fast approach to the power law observed in the magnetization and its second moment.

Another observation concerns the exponent b of the second moment. It turns out to be either weakly dependent on the temperature or even constant. It would be interesting to study the temperature dependence of this quantity also for other values of p and for the XY model ($p \to \infty$).

Our Monte Carlo estimates for $\eta(T)$ listed in Table I are consistent with earlier analytical and numerical work [13,18]. Since η is a derived quantity, its error bars are relatively large and with the present procedure it would be hard to obtain much smaller errors. However, we believe that these results confirm our basic hypothesis that the universal short-time behavior, previously known from Ising-like systems, also occurs in the KT phase. In particular this implies that there exists an exponent $\eta_0(T)$, the anomalous dimension of the initial magnetization, that in general is different from the exponent $\eta(T)$ of the static correlation function. This difference gives rise to the characteristic short-time behavior of the magnetization (1.1a) and also leaves its mark on the time dependence of the autocorrelation function $A(t)$ as expressed in (3.6).

ACKNOWLEDGMENTS

We should like to thank H. W. Diehl for reading the manuscript and useful comments. This work was supported in part by the Deutsche Forschungsgemeinschaft through Sonderforschungsbereich 237 "Unordnung und große Fluktuationen."

[1] H. K. Janssen, B. Schaub, and B. Schmittmann, Z. Phys. B **73**, 539 (1989).
[2] P. C. Hohenberg and B. I. Halperin, Rev. Mod. Phys. **49**, 435 (1977).
[3] H. W. Diehl and U. Ritschel, J. Stat. Phys. **73**, 1 (1993).
[4] The short-time exponent θ was denoted by θ' in Ref. [1]. But since the original θ of [1] does not appear in the present work, we have dropped the prime.
[5] Z.-B. Li, U. Ritschel, and B. Zheng, J. Phys. A **27**, L837 (1994).
[6] P. Grassberger, Physica A **214**, 547 (1995).
[7] Z.-B. Li, L. Schülke, and B. Zheng, Phys. Rev. Lett. **74**, 3396 (1995), and unpublished.
[8] L. Schülke and B. Zheng, Phys. Lett. A **204**, 295 (1995).
[9] H. K. Janssen, in *From Phase Transitions to Chaos — Topics in Modern Statistical Physics*, edited by G. Györgyi, I. Kondor, L. Sasvári, and T. Tel (World Scientific, Singapore, 1992).
[10] K. Oerding and H. K. Janssen, J. Phys. A **26**, 3369 (1993); **26**, 5295 (1993).
[11] H. K. Janssen and K. Oerding, J. Phys. A **27**, 715 (1994).
[12] J. M. Kosterlitz and D. J. Thouless, J. Phys. C **6**, 1181 (1973); J. M. Kosterlitz, *ibid.* **7**, 1046 (1974).
[13] V. José, L. P. Kadanoff, S. Kirkpatrick, and D. R. Nelson, Phys. Rev. B **16**, 1217 (1977); see also D. A. Nelson, in *Phase Transitions and Critical Phenomena*, edited by C. Domb and J. L. Lebowitz (Academic, London 1983).
[14] N. D. Mermin and H. Wagner, Phys. Rev. Lett. **22**, 1133 (1966).
[15] H. V. Roomany and H. W. Wyld, Phys. Rev. B **23**, 1357 (1981); P. Rujan, G. O. Williams, and H. L. Frisch, *ibid.* **23**, 1362 (1981).
[16] J. Tobochnik, Phys. Rev. B **26**, 6201 (1982); **27**, 6972 (1983).
[17] K. Kaski and J. D. Gunton, Phys. Rev. B **28**, 5371 (1983); K. Kaski, M. Grant, and J. D. Gunton, *ibid.* **31**, 3040 (1985).
[18] M. S. S. Challa and D. P. Landau, Phys. Rev. B **33**, 437 (1986).
[19] A. Yamagata and I. Ono, J. Phys. A **24**, 265 (1991).
[20] Y. Leroyer and K. Rouditi, J. Phys. A **24**, 1931 (1991).
[21] M. Mondello and N. Goldenfeld, Phys. Rev. A **42**, 5865 (1990).
[22] B. Yurke, A. N. Pargellis, T. Kovacs, and D. A. Huse, Phys. Rev. E **47**, 1525 (1993).
[23] R. E. Blundell and A. J. Bray, Phys. Rev. E **49**, 4925 (1994); A. J. Bray and A. D. Rutenberg, *ibid.* **49**, R27 (1994).

[24] Throughout this paper we use the "magnetic" language. The term "order parameter" is sometimes used as a synonym for "magnetization" (density) and does not mean any form of topological order, which would characterize the difference between *equilibrium* states above and below T_{KT}.

[25] Since we identify $\eta/2$ with the scaling dimension of the field, all formulas presented in Sec. III are restricted to $d = 2$. But it is straightforward to extend the analysis to general spatial dimension.

[26] D. A. Huse, Phys. Rev. B **40**, 304 (1989).

[27] U. Ritschel and H. W. Diehl (unpublished).

[28] U. Ritschel and H. W. Diehl, Phys. Rev. E **51**, 5392 (1995).

[29] J. M. Sancho, M. San Miguel, and J. D. Gunton, J. Phys. A **13**, L443 (1980).

[30] K. Binder and D. W. Heermann, *Monte Carlo Simulation in Statistical Physics* (Springer-Verlag, Berlin, 1988).